Physicochem. Probl. Miner. Process., 61(5), 2025, 213637

http://www.journalssystem.com/ppmp

Physicochemical Problems of Mineral Processing

ISSN 1643-1049

Effect of gangue minerals on apparent viscosity and flotation of coal slime

Tingshun Wang [1,3,4], Jianghe Wang [1,3,4], Xianbo Li [1,3,4], Qin Zhang [2,3,4]

[1] Mining College, Guizhou University, Guiyang 550025, Guizhou, China

[2] Guizhou Academy of Sciences, Guiyang 550001, Guizhou, China

[3] National & Local Joint Laboratory of Engineering for Effective Utilization of Regional Mineral Resources from Karst Areas, Guiyang 550025, Guizhou, China

[4] Guizhou Key Lab of Comprehensive Utilization of Non-metallic Mineral Resources, Guiyang 550025, Guizhou, China

Corresponding author: zq6736@163.com (Qin Zhang)

Abstract: In coal slime flotation, non-selective aggregation between fine gangue minerals and coal particles is a critical factor leading to the deterioration of coal floatability and a reduction in clean coal recovery. This study investigated the influence of three minerals commonly found in coal, quartz, kaolinite, and muscovite, on apparent viscosity and coal floatability. The results demonstrate that as the amount of gangue minerals increased, the apparent viscosity of the pulp increased to varying extents. Quartz exhibited the least impact on apparent viscosity, followed by kaolinite, while muscovite had the most significant effect. The addition of quartz, kaolinite, and muscovite decreased the flotation recovery from 79.46% to 74.09%, 62.50%, and 54.96%, respectively. The projected area of coal particles attached to bubbles decreased by 10.03%, 19.16%, and 30.14% compared to the blank test. These findings are consistent with the apparent viscosity results. Extended DLVO theoretical analysis revealed that the electrical double-layer repulsive forces between coal and quartz/kaolinite overcame the attractive van der Waals and hydrophobic forces, resulting in net repulsive interactions. In contrast, the net interaction force between coal and muscovite remained attractive under the experimental conditions, facilitating their aggregation and thereby impairing coal floatability. This observation aligns with the flotation and bubble-particle adhesion test outcomes. The study provides a theoretical foundation for regulating apparent viscosity in coal slime flotation and achieving efficient separation between coal and gangue minerals.

***Keywords*:** coal slime flotation, gangue minerals, apparent viscosity, bubble-particle adhesion, extended DLVO

1. Introduction

Coal, the most abundant and widely distributed fossil fuel resource globally, continues to be the dominant energy source in China both currently and for the foreseeable future. This prominence is primarily driven by the nation's distinctive geological endowment of fossil energy resources, characterized by an abundance of coal, relative scarcity of oil, and scarcity of natural gas. Consequently, coal's central position within China's energy mix is expected to remain largely unchanged in the near term (Huang and Xu et al., 2020; Li and Xia et al., 2020; Lin and Mei et al., 2022; Gao and Li et al., 2024). Flotation represents a critical unit operation for coal beneficiation, primarily aimed at substantially reducing ash content to enhance the calorific value and, consequently, the commercial value of the clean coal product. The core principle underpinning coal flotation exploits the pronounced difference in surface hydrophobicity between valuable coal particles and gangue minerals. Separation is achieved via bubble-particle attachment: natural hydrophobic coal particles preferentially adsorb onto air bubbles and are transported to the pulp surface, forming a mineral-laden froth concentrate rich in combustible matter. Conversely, hydrophilic gangue minerals, which harbor the majority of the ash-forming constituents, are predominantly rejected to the pulp phase and report to the tailings stream. It is noteworthy that common gangue minerals present in coal slimes, such as quartz, kaolinite, and

DOI: 10.37190/ppmp/213637

muscovite, can engage in complex solid-liquid interfacial interactions with coal particles within the pulp system. Detrimental mechanisms, including mechanical water entrainment and slime coating, can then significantly impede the separation efficiency (Xing and Xu et al., 2017; Li and Liang et al., 2022; Zhu and Zhao et al., 2025). Consequently, these gangue minerals report to the clean coal product, contaminating it and thereby compromising flotation performance by reducing the ultimate combustible recovery (Yu and Ma et al., 2017; Ni and Bu et al., 2018; Li and Zhang et al., 2023).

The adverse effects stemming from interactions between gangue minerals and coal particles are frequently manifested in pulp rheological properties. Rheology, the study of the deformation and flow behavior of materials under applied stress, forms the theoretical basis for analyzing the dynamics of mineral pulps. These heterogeneous solid-liquid suspensions comprise dispersed mineral particles and water. Rheological characterization effectively quantifies the intensity of inter-particle interactions and the degree of particle aggregation within the pulp, both parameters exhibiting a significant correlation with flotation performance. Yield stress and apparent viscosity constitute two key rheological parameters for characterizing pulp rheological behavior (Wang and Li, 2020). These parameters provide essential quantitative indicators for evaluating the strength of inter-particle forces and the particle dispersion state within the pulp. Apparent viscosity has been widely adopted as an effective parameter for characterizing particle interactions across various mineral systems, including oxide ores (Chen and Chen et al., 2019; Shang and Sun, 2023), sulfide minerals (Gao and Zhang et al., 2018; Liu and Zhang et al., 2021), clay minerals (Zhang and Peng, 2015; Cruz and Peng, 2016; Farrokhpay and Ndlovu et al., 2016; Wang and Mu et al., 2024), and coal slurries (Li and Deng et al., 2017; Zhang and Cao et al., 2017; Guo and Huang et al., 2023). Studies have shown that the presence of clay minerals has a significant effect on slurry rheology and mineral recovery during flotation. Basnayaka et al. (Basnayaka and Subasinghe et al., 2017) pointed out that well-dispersed clay minerals can significantly change the rheological properties of the slurry and lead to a decrease in the recovery rate of pyrite. Cruz et al. (Cruz and Peng et al., 2015) found that adding lime to the pulp can increase its apparent viscosity, thereby increasing the mechanical entrainment of copper and gold, resulting in a decrease in concentrate grade. In addition, the study of Chen et al. (Chen and Zhao et al., 2020) showed that montmorillonite can significantly increase the viscosity of the pulp, thus seriously inhibiting the flotation effect of pyrite. There exists a direct correlation between pulp rheological behavior and flotation performance (Sajjad and Otsuki, 2022b; Zhao and Zhang, 2024). Increased pulp viscosity requires higher shear stress to rupture particle networks, subsequently dampening turbulence intensity, compromising gas dispersion uniformity, restricting particle and bubble mobility, and diminishing bubble-particle collision frequency - all critical determinants of flotation performance (Das and Kelly et al., 2011; Wang and Peng et al., 2016). Collectively, these mechanisms degrade key flotation performance indicators.

During coal flotation, gangue mineral particles in the pulp readily undergo non-selective adsorption and aggregation with coal particles, substantially elevating apparent pulp viscosity. This increased viscosity directly compromises flotation efficiency through two mechanisms: air bubbles become obstructed by gangue-derived spatial networks or entrained by fine slimes, while simultaneously, enhanced turbulent damping reduces bubble-particle collision efficiency. Consequently, maintaining low pulp viscosity is essential for achieving efficient coal-gangue separation (Li and Zhao et al., 2019; Wang and Zhu et al., 2020; Kumar and Arora, 2022). A low-viscosity pulp environment minimizes turbulent damping, enhancing particle-bubble collision probability and coal floatability. This confirms pulp rheology control as fundamental for optimizing flotation efficiency, providing both theoretical grounding and a high-performance pathway for intensified coal-gangue separation. Although it has become a consensus that clay minerals generally have a negative impact on the flotation process, their specific mechanism of action has not been fully elucidated. In recent years, rheology has been increasingly used as an effective tool to explain the flotation mechanism and optimize the flotation process through rheological adjustment. However, in the field of coal flotation research, systematic research on how gangue minerals affect apparent viscosity and flotation is still relatively limited, especially based on different gangue minerals. Therefore, this study aims to fill this research gap and deeply analyze the influence mechanism of gangue minerals in the process of coal slime flotation. This study has important theoretical guiding significance for revealing the interaction mechanism between gangue minerals and coal particles in the slurry, and finally achieving efficient separation control.

This study investigates the influence of major coal gangue minerals, quartz, kaolinite, and muscovite, on pulp rheological properties and flotation behavior. By systematically examining the effects of exogenous mineral addition on rheological parameters and flotation performance indicators, combined with apparent viscosity measurements, bubble-particle attachment analysis, and Extended DLVO theoretical analysis, we quantitatively characterize interparticle interaction strengths within the pulp

system. The research elucidates evolution patterns in the aggregation/dispersion states of mineral-coal particle systems, providing a theoretical framework for mitigating gangue mineral contamination mechanisms in fine coal flotation and establishing a scientific foundation for enhancing clean coal concentrate recovery efficiency.

2. Materials and methods

2.1. Materials

Coal samples were sourced from the flotation feed of a Guizhou Province coal preparation plant. To obtain high-purity material and eliminate non-target interference, the raw coal was screened to remove particles larger than 0.5 mm and subsequently upgraded via a shaking table concentration. The coal sample had a low ash content of 5.98% and a moisture content of 1.68%. The volatile matter content was 25.56%, and the fixed carbon content was 74.44% (Table 1). X-ray photoelectron spectroscopy (XPS, Fig. 1a) analysis of the clean coal revealed a dominant carbon content (91.26%), with oxygen at 6.79% and combined aluminum/silicon totaling only 1.95%. This minimal surface oxygen functionality and hydrophilic mineral content preclude interference from impurities and surface chemistry in subsequent studies. Complementary gangue minerals comprised quartz (Henan Mishang Environmental Protection Technology Co., Ltd.), kaolinite, and muscovite (Shanlin Stone Language Co., Ltd.). All experiments were conducted using deionized (DI) water with an electric resistivity of 18.25 MΩ·cm. Particle size analysis of the coal sample (LS13320 laser analyzer, Fig. 1b) showed the coal had a volume mean diameter of 61.10 μm. Additionally, quartz, kaolinite, and muscovite exhibited volume mean diameters of 16.08 μm, 14.83 μm, and 12.28 μm, respectively. X-ray diffraction (XRD, Fig. 2) confirmed high crystalline purity for all minerals, satisfying requirements for interaction studies. This rigorous control over particle size and purity distribution effectively eliminates coupled interference from extraneous minerals and size effects on solid-liquid interface phenomena.

Table 1. Proximate analysis of the coal samples

Parameter	M_{ad}	A_{ad}	V_{daf}	FC_{daf}
Content (%)	1.68	5.98	25.56	74.44

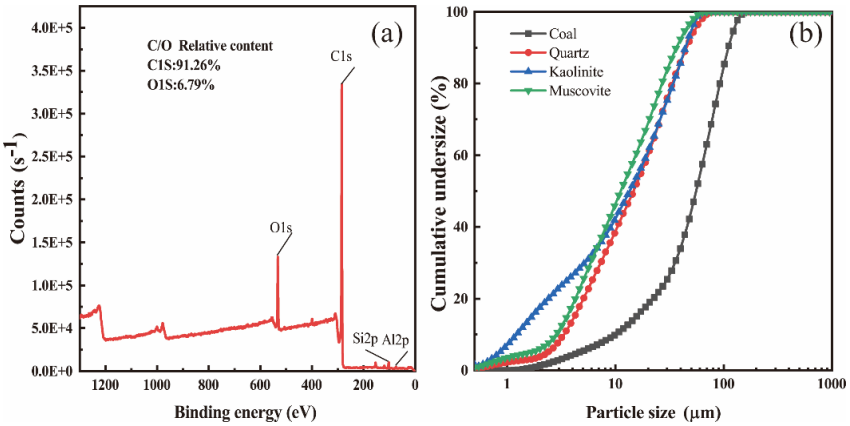

Fig. 1. (a) XPS energy spectrum of coal surface, and (b) particle size distribution of coal, quartz, kaolinite, and muscovite samples

2.2.1. Zeta potential measurements

The zeta potential values of coal, quartz, kaolinite, and muscovite samples were measured using a Zetasizer Delsa Nano C system (Beckman Coulter, U.S.A.). The samples were ground to less than 30 μm using a three-head agate grinder. A 50 mg of each sample was weighed and placed in 1.0 dm^3 of 0.1 mmol/dm^3 NaCl (Chengdu Jinshan Chemical Reagent Co., Ltd., with a purity of more than 99.5%) solution at pH 7.5. Which was used to facilitate the calculation of interparticle forces based on the EDLVO theory. After ultrasonic treatment for 2 min, the suspension was stirred uniformly to ensure the thorough dispersion of the mineral particles. The supernatant of the fine particle suspension was used for the zeta potential measurements. The measurement was repeated three times; the measurements had an average error margin ranging between approximately 0.25 and 1.31, and the average value was taken as the final result.

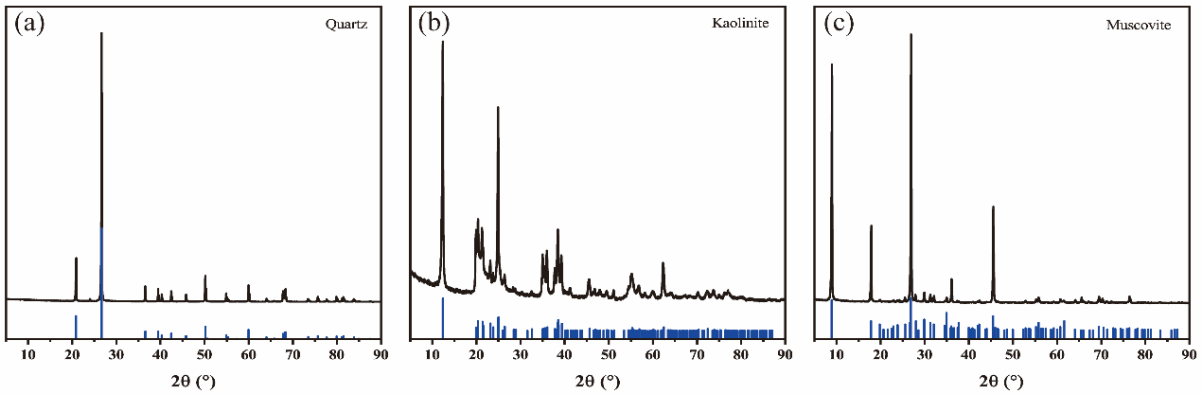

Fig. 2. XRD patterns of (a) quartz, (b) kaolinite, and (c) muscovite

2.2. Methods

2.2.2. Contact angle measurements

The coal, quartz, kaolinite, and muscovite samples used in the experiment were all less than 30 μm in particle size. The contact angle of the samples was measured using the plate pressing method, with a pressing pressure of 20 MPa. The contact angle of the samples was measured in water, glycerol, and formaldehyde, respectively. During the measurement, the samples were fixed on the test stand. Using a micro syringe, 2μL of DI water was slowly dispensed to contact the mineral surface. When the droplet had spread on the surface for 5 seconds, the contact angle was automatically measured by the instrument. Each sample was tested three times at different positions, and the average value was taken as the final data.

2.2.3. Bubble-particle adhesion characterization

A bubble-particle adhesion testing system was constructed to measure bubble-particle adhesion. The equipment's principle diagram is shown in Fig. 3. The testing apparatus consists of a computer, camera, light source, capillary tube, micro syringe pump, quartz cuvette (3.5 × 3.5 × 5 cm), and magnetic stirrer. 0.35 g of coal and 0.15 g of mineral particle sample, and 40 mL of deionized water to the quartz cuvette. The solution was first thoroughly mixed using a magnetic stirrer at 500 rpm for 5 min. After stirring was stopped, the slurry was allowed to settle. A bubble with a diameter of approximately 3 mm was then generated at the bottom of the capillary tube using a micro-syringe pump. Subsequently, the slurry was mixed again at 250 rpm for 30 seconds. After stirring ceased, some coal particles settled to the bottom of the glass chamber, while others adhered to the bubble surface. Images of the bubble with stably adhered particles were captured. The cross-sectional area of the particles on the bubble was analyzed using these images with ImageJ software to characterize the bubble's loading capacity.

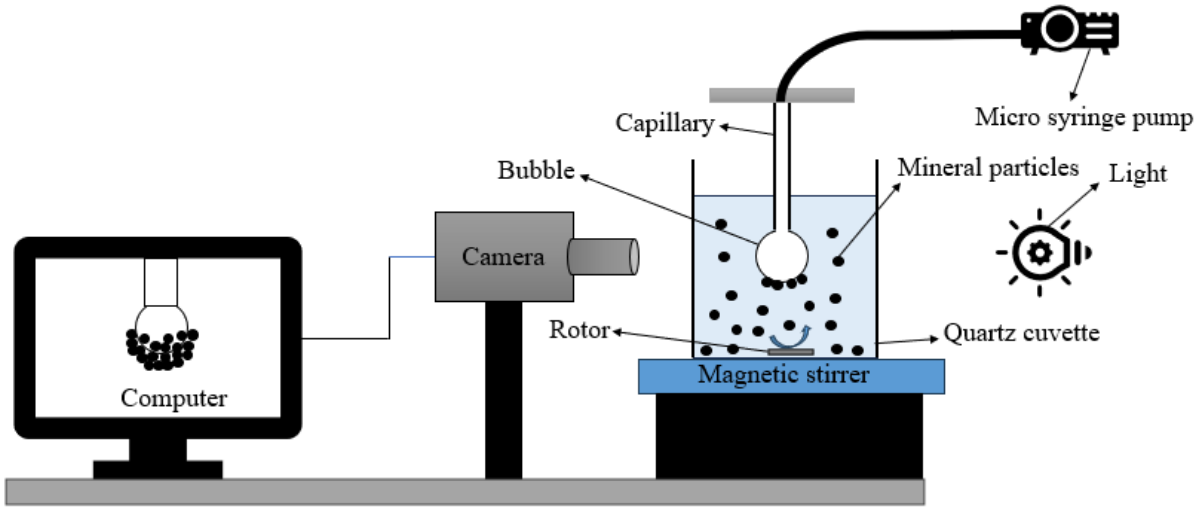

Fig. 3. Bubble-particle adhesion test system schematic diagram

2.2.4. Apparent viscosity analysis

Apparent viscosity analysis was conducted using a Brookfield DVnext rheometer. To investigate the effects of quartz, kaolinite, and muscovite on the rheological properties of coal slurry, the slurry was prepared by adding 10 %, 20 % and 30 % of coal and minerals. The slurry was stirred for 30 s, and then the viscosity of the slurry was measured. Each group of slurry was tested for 20 s, with three sets of data measured and averaged. Apparent viscosity was tested at room temperature, with the temperature maintained around 25°C. An appropriate rotor was selected, and the rotor was fully immersed in the slurry for rheological testing. The torque range of the rotor used for rheological testing was maintained between 10% and 100%. For unknown fluids, the selection of the rotor and speed required repeated experiments, and based on the experimental results, the LV61 rotor was ultimately chosen.

2.2.5. Flotation experiments

Floating experiments were conducted using a flotation machine ($XFGC_{II}$-5 ~ 35 g, Jilin prospecting machinery factory, China) with a 100 cm^3 capacity and an impeller speed of 1992 rpm to study the effects of quartz, kaolinite, and muscovite on coal flotation performance. A stirrer was used to disperse 5.6 g of coal particles with a particle size of 0.125–0.07 mm and 2.4 g of mineral particles with a particle size less than 0.074 mm in 50 cm^3 of deionized water. The mixture was stirred at 1000 rpm for 10 min to ensure sufficient collision and contact between the coal and minerals. Simultaneously, when 5.6 g of coal with an ash content of 5.98% was mixed with 2.4 g of mineral particles smaller than 0.074 mm, the average ash content of the mixed solid particles was approximately 34.19%, which is close to the ash content of the actual raw coking coal.

After stirring, the slurry was transferred to a 100 cm^3 flotation cell, with a flotation slurry concentration of 80 g/dm^3. The slurry was adjusted for 2 min, and flotation reagents were added. Kerosene was used as a collector, with a dosage of 100 g/Mg; the frother used was methyl isobutyl carbinol (MIBC), with a dosage of 50 g/Mg, and the flotation time was kept at 2 min. After flotation, the flotation concentrate slurry was wet-screened using a 0.074 mm sieve. Particles larger than 0.074 mm were considered coal particles, while mineral particles less than 0.074 mm were concentrated in the undersize fraction. In this experiment, both pulp preparation time and flotation duration were relatively short, with agitation intensity primarily optimized to maintain particle dispersion. Consequently, the generation of particles less than 0.074 mm in size was relatively limited during coal flotation. Since coal particles with ash content as low as 5.98% were used in this study, only the recovery of the solid matter was considered. The solid matter recovery (R_t) was calculated based on Eq. (1), and the mineral mass recovery (R_m) was calculated based on Eq. (2).

$$R_t = 100(m_1 + m_2)/m_t \tag{1}$$

$$R_m = 100m_2/m_t \tag{2}$$

where m_1 represents the mass of coal particles in the concentrate, m_2 represents the mass of mineral particles entering the flotation concentrate foam, and m_t represents the total feed mass.

2.2.6. Calculation the interaction energy between coal and mineral particles using EDLVO theory

The interaction force between coal and quartz, kaolinite, and muscovite in slurry was studied, and the aggregation and dispersion mechanism of mineral particles in slurry fluid was revealed, so as to clarify the influence of rheological properties on coal slime flotation. The total interaction energy (V_T) between colloidal particles can be obtained using Eq. (3):

$$V_T = V_w + V_E + V_H \tag{3}$$

In Eq. (3), V_W, V_E, and V_H represent the interparticle van der Waals energy, double layer energy, and polar interface interaction energy, respectively.

2.2.6.1. Interparticle van der Waals energy (V_W)

V_W can be calculated using Eq. (4):

$$V_W = -\frac{A_{132}}{6h}\frac{R_1R_2}{R_1+R_2} \tag{4}$$

here R_1 and R_2 are the particle sizes of the two mineral particles, respectively; h is the interaction distance between particles; A_{132} is the effective Hamaker constant for the interaction between substance 1 and substance 2 in the third medium, calculated using Eq. (5).

$$A_{132} = (A_{11} - A_{33})(A_{22} - A_{33}) \quad (5)$$

where A_{11}, A_{22}, and A_{33} are the Hamaker constants of substance 1, substance 2, and medium 3 in a vacuum, respectively. The Hamaker constants of the four minerals coal, quartz, kaolinite, and muscovite, as well as the medium water, are shown in Table 2 (Tang and Zhang et al., 2016; Chen and Wang et al., 2018; Yu and Ma et al., 2018).

Table 2. The Hamaker constants of minerals and water

Materials	Coal	Quartz	Kaolinite	Muscovite	Water
A (10^{-20}J)	6.07	6.30	8.60	9.86	3.70

2.2.6.2. Electrostatic double layer energy (V_E)

Eq. (6) determines the electrostatic double layer energy

$$V_E = \frac{\pi\varepsilon\varepsilon_0 R_1 R_2}{R_1+R_2}[2\varphi_1\varphi_2 ln\frac{1+e^{-\kappa h}}{1-e^{-\kappa h}} + (\varphi_1^2 + \varphi_2^2)\ln(1 - e^{-2\kappa h}] \quad (6)$$

where ε is the relative permittivity of a 0.1 mmol/L NaCl solution, taken as 78.5 $C^2 \cdot m/J$; ε_0 is the permittivity of free space, taken as 8.854×10^{-12} $C^2 \cdot m/J$; φ_1 and φ_2 are the surface potentials of substance 1 and substance 2, respectively, replaced by the measured zeta potential values. The Zeta potential values for coal, quartz, kaolinite, and muscovite are shown in Table 3. For a 0.1 mmol/L NaCl solution at 25 °C, the Debye length is 30.4 nm (Li and Xia et al., 2019).

Table 3. Zeta potential measurement results of coal and gangue particles

Sample	Coal	Quartz	Kaolinite	Muscovite
Zeta potential (mV)	-7.36	-29.80	-23.63	-0.36

2.2.6.3. Polar interface interaction energy (V_H)

For systems with fine particles and coarse particles with large differences in particle size, the interaction model between spheres and plates is selected:

$$V_H = 2\pi\frac{R_1 R_2}{R_1+R_2} h_0 V_H^0 e^{\frac{H_0-h}{h_0}} \quad (7)$$

where H_0 is the equilibrium contact distance between the surfaces of the two mineral particles, approximately 0.2 nm; h_0 is the decay length, approximately 1 nm (Deng and Yang et al., 2019); and where V_H^0 is the polar interface interaction energy constant, which can be calculated using Eq. (8):

$$V_H^0 = 2[\gamma_3^+\sqrt{\gamma_1^-} + \gamma_2^{-\sqrt{\gamma_3^-}} + \sqrt{\gamma_3^+}\left(\sqrt{\gamma_1^+} + \sqrt{\gamma_2^+} - \sqrt{\gamma_3^+}\right) - \gamma_1^+\gamma 2 — \sqrt{\gamma_1^-\gamma_2^+}] \quad (8)$$

where γ_1^+, γ_2^+, and γ_3^+ are the electron acceptor components of the surface energy of substance 1, substance 2, and medium 3, respectively, while γ_1^-, γ_2^-, and γ_3^- are the electron donor components of the surface energy of substance 1, substance 2, and medium 3, respectively.

For water media, γ_3^+ and γ_3^- are known quantities, while γ_1^- and γ_2^- can be calculated using Eq. (9):

$$(1 + cos\theta)\gamma_L = 2(\sqrt{\gamma_s^d\gamma_L^d} + \sqrt{\gamma_s^+\gamma_L^-} + \sqrt{\gamma_s^-\gamma_L^+}) \quad (9)$$

where γ_L is the surface energy of the liquid, γ_L^d is the dispersion component of the liquid surface energy, and γ_s^d is the dispersion component of the solid surface energy; γ_s^+ is the electron acceptor component of the solid surface energy; γ_s^- is the electron donor component of the solid surface energy; θ is the contact angle of the solid particle surface. Table 4 lists the surface energy parameters for water, glycerol, and formaldehyde, while Table 5 lists the contact angles of coal, quartz, kaolinite, and muscovite in different liquids.

Table 4. Surface energy parameters of water, glycerol, and formaldehyde

Liquids	γ_L (mJ/m²)	γ_L^d (mJ/m²)	γ_L^+ (mJ/m²)	γ_L^- (mJ/m²)
Water	72.8	21.8	25.5	25.5
Glycerol	64.0	34.0	4.92	57.4
Formaldehyde	58.0	39.0	2.28	39.6

Table 5. Contact angles of coal, quartz, kaolinite, and muscovite

Liquids and solid samples	Contact angle (°)			
	Coal	Quartz	Kaolinite	Muscovite
Water	67.7	18.6	26.5	17.7
Glycerol	52.8	28.9	37.6	28.2
Formaldehyde	38.9	15.8	23.1	15.3

3. Results and discussions

3.1. Effect of the amount of gangue minerals on apparent viscosity

The effects of gangue minerals on the rheological properties of the slurry are shown in Fig. 4. As seen in Fig. 4, the viscosity of the mixed slurry containing quartz, muscovite, kaolinite, and coal increases with increasing shear rate, regardless of the amount of each mineral added. The slurry exhibits expansive fluid behavior. Quartz has the least effect on the rheological properties of the pulp, as it is an oxide mineral with highly stable physical and chemical properties, exerting only a weak influence on apparent viscosity. Kaolinite and muscovite, being clay minerals, have a stronger impact on apparent viscosity. Muscovite has a more significant effect on the rheology of the slurry than kaolinite, which may be because muscovite particles form a three-dimensional network structure in the slurry through face-to-layer and face-to-face bonding (Yan and Englert et al., 2011).

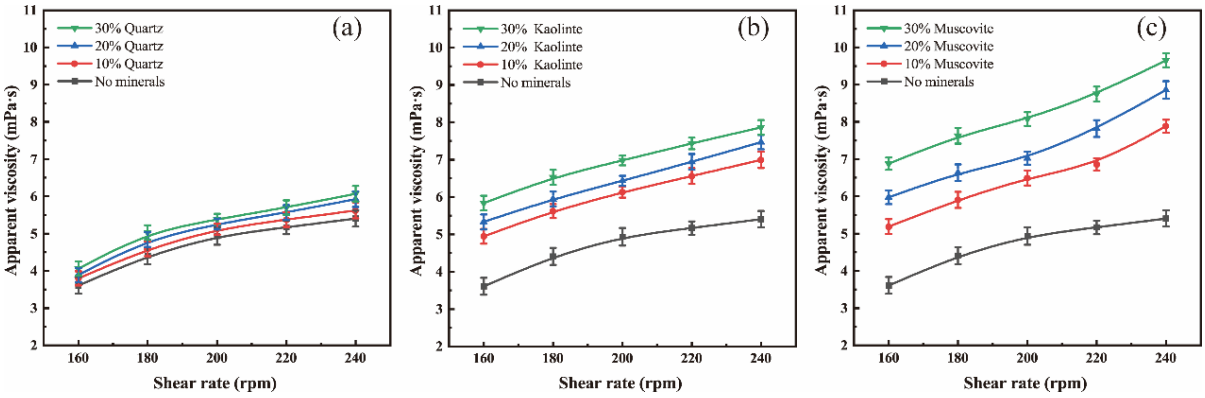

Fig. 4. The effect of different dosages of (a) quartz, (b) kaolinite, and (c) muscovite on apparent viscosity

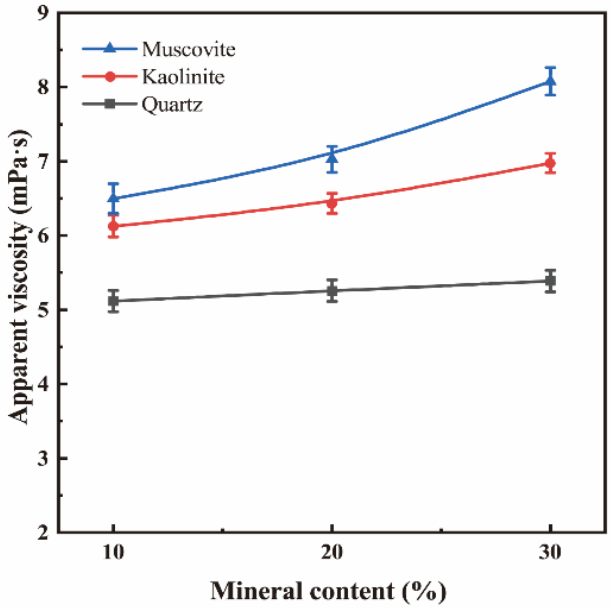

Fig. 5. The effect of mineral content on apparent viscosity at a shear rate of 200 rpm

Fig. 5 shows the effect of quartz, kaolinite, and muscovite mineral content on apparent viscosity at a shear rate of 200 rpm. As the amount of mineral additives increases, the apparent viscosity of all pulp increases, but the increase in apparent viscosity varies greatly. The apparent viscosity of quartz does not change significantly with increasing additive amounts, while increasing the amounts of kaolinite and muscovite has a greater effect on apparent viscosity. As the additive amounts increase, the addition of kaolinite and muscovite causes the apparent viscosity of the pulp to increase rapidly. When the addition rate is 30%, the apparent viscosity of the kaolinite and muscovite pulp is 6.97 and 8.08 mPa·s, respectively, while the apparent viscosity of the quartz pulp is 5.19 mPa·s. The apparent viscosities increased by 1.78 and 2.89 mPa·s, respectively. The apparent viscosities of the kaolinite and muscovite slurries were 1.3 and 1.6 times that of the quartz slurry. These results are consistent with those reported by Wang et al. (Wang and Zhang et al., 2020), who indicated that an increase in the addition of fine gangue minerals significantly reduces the flotation recovery rate of the target mineral, with the extent of this effect being closely related to the mineral type.

3.2. Flotation experiments

Figure 6 shows the comparative flotation performance of the coal sample with and without gangue mineral additions. In the absence of mineral particles, the solid matter recovery reached 79.46%. Conversely, coal-quartz blends achieved 74.09% recovery, while coal-kaolinite and coal-muscovite systems exhibited progressively lower recoveries of 62.50% and 54.96%, respectively. The results indicate that the addition of muscovite showed the greatest impact on the flotation effect of coal, followed by kaolinite and quartz. Additionally, the mineral mass recovery (R_m) of coal mixed with quartz, kaolinite, and muscovite is 11.30%, 9.32%, and 15.67%, respectively. This phenomenon suggests that more muscovite particles enter the flotation concentrate foam compared to quartz and kaolinite. The solid matter recovery (R_t) and mineral mass recovery (R_m) also suggest that quartz, kaolinite, and muscovite may enter the flotation concentrate foam through mechanisms such as fine slime coverage and water flow entrainment. During the flotation process, non-selective adsorption and aggregation may occur between kaolinite, muscovite, and coal particles (Hu and Liang et al., 2019; Li and Zhang et al., 2020), and these effects may reduce the flotation recovery rate of coal.

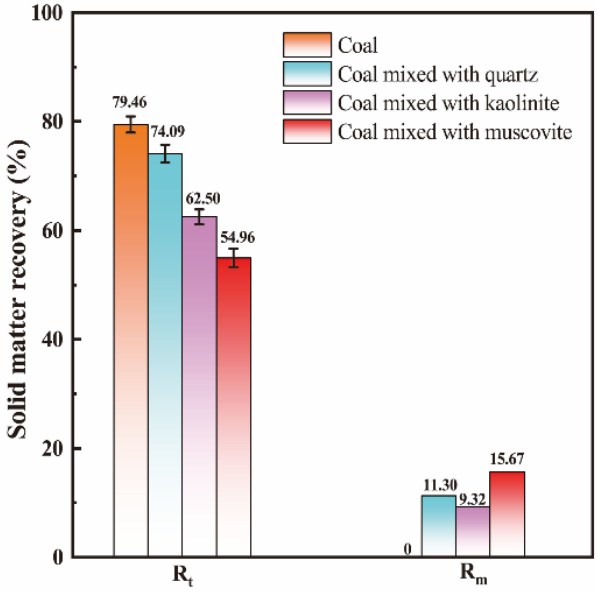

Fig. 6. Solid matter recovery of coal particles with and without mineral particles

3.3. Adhesion between coal particles and bubbles

Bubble-particle load images were processed using ImageJ software. To measure the cross-sectional area of coal particles adhering beneath bubbles, images were first converted to 8-bit grayscale. Spatial calibration was performed on each image using the built-in scale, converting pixel values to actual bubble dimensions (3mm). Subsequently, the "Irregular Shape" tool is used to manually select the outline of the bubble enveloped by coal particles, determining its complete projected area. Particle regions are precisely identified by manually adjusting the threshold. Finally, the "ROI Manager" tool

calculates the enveloped cross-sectional area. This metric reflects the coal's flotation performance; the measurement was repeated three times, and the average value was taken as the final result. Figs. 7 and 8 present the bubble load test results for coal mixed with quartz, kaolinite, and muscovite for 30 seconds. The baseline test (no mineral addition) yielded a maximum adhering coal particle area of 2.6223 mm². Upon adding quartz, the loaded coal particle area decreased to 2.3591 mm², representing a 10.03% reduction compared to the baseline. The addition of kaolinite further reduced the loaded area to 2.1199 mm² (a 19.16% decrease). Muscovite addition exerted the most significant effect, reducing the loaded coal particle area to 1.8320 mm², a decrease of 30.14% relative to the baseline.

This demonstrates the influence of three minerals on the floatability of coal particles, namely that quartz has the least influence on the floatability of coal particles, kaolinite has the second least influence, and muscovite has the greatest influence, which is consistent with the results of flotation experiments.

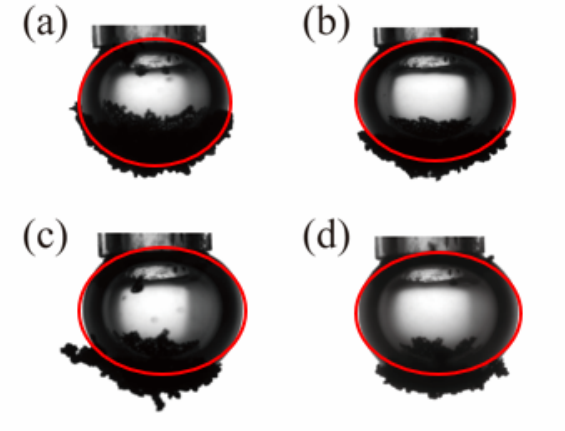

Fig. 7. Adhesion of coal particles to bubble surfaces for coal mixed with (a) no mineral, (b) quartz, (c) kaolinite, and (d) muscovite

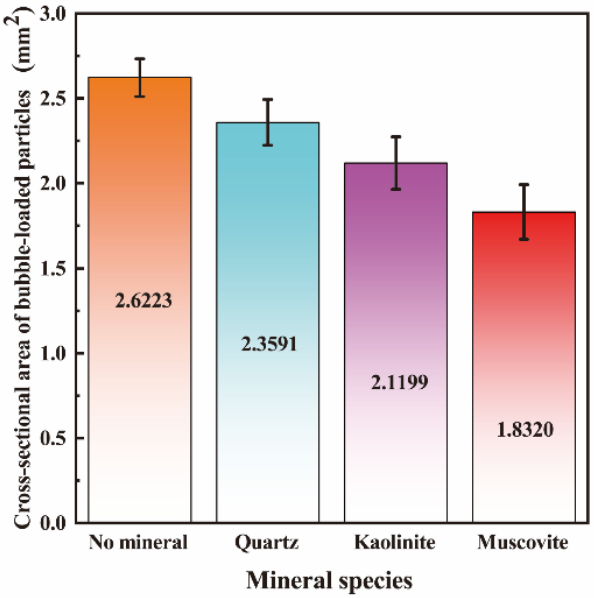

Fig. 8. Influence of different minerals on the bubble loading of coal particles after mixing for 30s

3.4. Interaction energy between coal and mineral particles

Figures 9(a)-(c) demonstrate that the van der Waals energy and polar interfacial interaction energy between coal and quartz, kaolinite, and muscovite are consistently negative (attractive) across the interaction distance, with minimal variation between minerals. As the separation distance increases, the double-layer interaction between coal particles and both quartz and kaolinite transitions from attraction to repulsion. The double-layer repulsion between coal and quartz exceeds that between coal and kaolinite, with both forces decaying gradually with increasing distance. In contrast, coal and muscovite exhibit exclusively attractive interactions across the entire distance range.

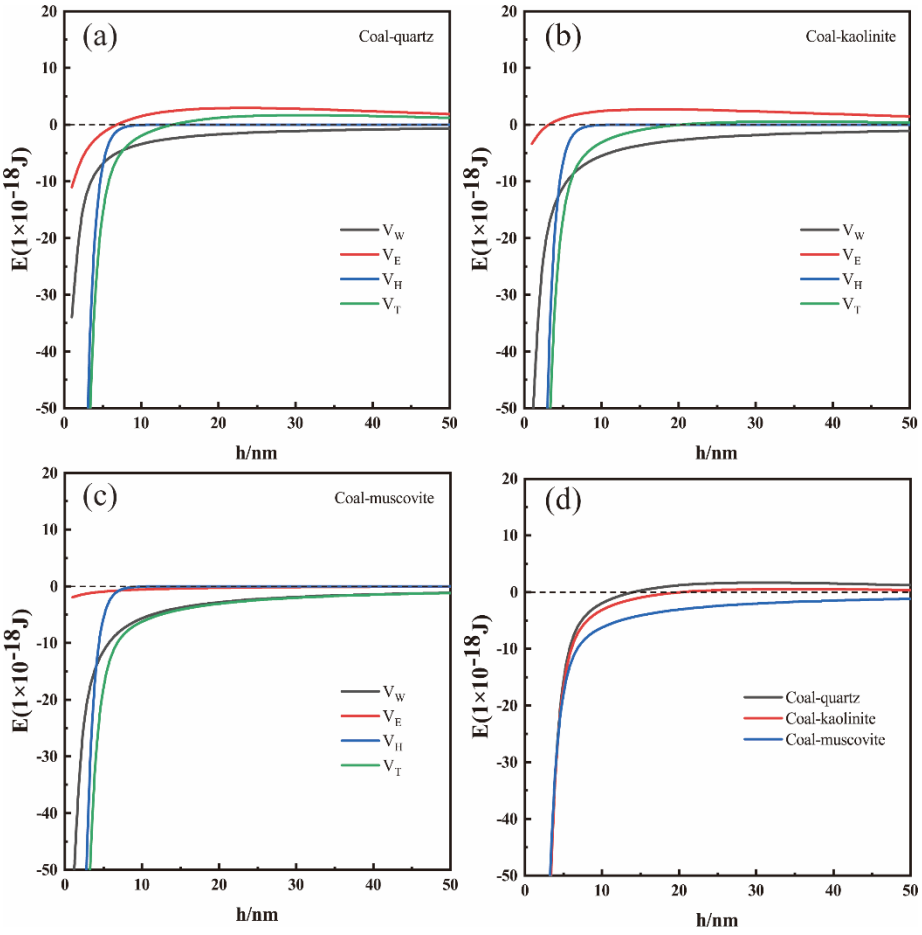

Fig. 9. The interaction energy between coal and (a) quartz, (b) kaolinite, (c) muscovite, and (d) the total interaction energy between coal and the three minerals was calculated using EDLVO theory

The total interaction energy profiles (Fig. 9d) confirm this behavior, showing decreasing magnitudes with greater interparticle separation. A distinct energy barrier emerges for coal-quartz and coal-kaolinite systems at approximately 18 nm, where the net interaction shifts from attractive to repulsive. This transition occurs when the repulsive double-layer forces overcome the combined van der Waals and hydrophobic attraction. Notably, the repulsive barrier is higher for quartz than for kaolinite. Conversely, the total interaction energy between coal and muscovite remains attractive at all separations. These energy profiles elucidate the distinct aggregation behaviors: muscovite's persistent attraction promotes hetero-aggregation with coal under experimental conditions, directly impacting coal floatability. This mechanistic interpretation aligns consistently with observed apparent viscosity and flotation test results.

In the flotation process, the rheological properties of the pulp are the macroscopic reflection of the interaction at the micro level, including the interaction between different particles and the interaction between particles and water. In fact, by analyzing the rheological properties of the pulp, the degree of interaction or aggregation of particles in the pulp can be evaluated. There is a close relationship between pulp viscosity and flotation performance. Different pulp apparent viscosity has a different flotation effect (Farrokhpay, 2012; Liu and Cui et al., 2024). Fig. 10 shows a schematic mechanism of particle dispersion and bubble-particle adhesion states in pulp. In the mixed slurry of coal and quartz, the apparent viscosity of the slurry is low, and the dispersion state between particles is good. The lower slurry viscosity is beneficial to improve the collision efficiency between particles and bubbles, which can improve the floatability of coal particles in the slurry. In the mixed slurry of coal, kaolinite, and muscovite, the apparent viscosity of the slurry increases to varying degrees. Compared with kaolinite, muscovite has a greater influence on the apparent viscosity of the pulp. Jeldres et al. (Jeldres and Uribe et al., 2019) demonstrated that both viscosity and yield stress become predominant factors governing the fluid dynamics of mineral pulp systems when fine clay minerals are present. When there are clay minerals such as kaolinite and muscovite in the slurry, their unique layered crystal structure is easy to hydrate, expand, and disperse in the slurry, and form a network aggregate structure through complex

interactions between particles. This will greatly increase the apparent viscosity of the pulp. In order to alleviate the adverse effects of high viscosity, targeted measures can be taken to improve the rheology in practice. For example, the flocculation structure between particles is destroyed by adding dispersants such as sodium hexametaphosphate and water glass, or the aggregates are destroyed by mechanical means such as high shear slurry adjustment and ultrasonic pretreatment. Pre-desliming can also be considered to reduce the content of easily mudded minerals from the source (Chen and Peng, 2018; Li and Zhang et al., 2025). The deterioration of this rheological property will lead to a significant decrease in the turbulence intensity of the slurry and increase the movement resistance of bubbles and particles, which not only seriously hinders the effective mineralization of bubbles and the selective adhesion of coal particles, but also aggravates the non-selective cover and mechanical entrainment of gangue minerals on the surface of coal particles, and finally has a strong inhibitory effect on the floatability of coal particles. These adverse effects will reduce the floatability of coal particles in the slurry.

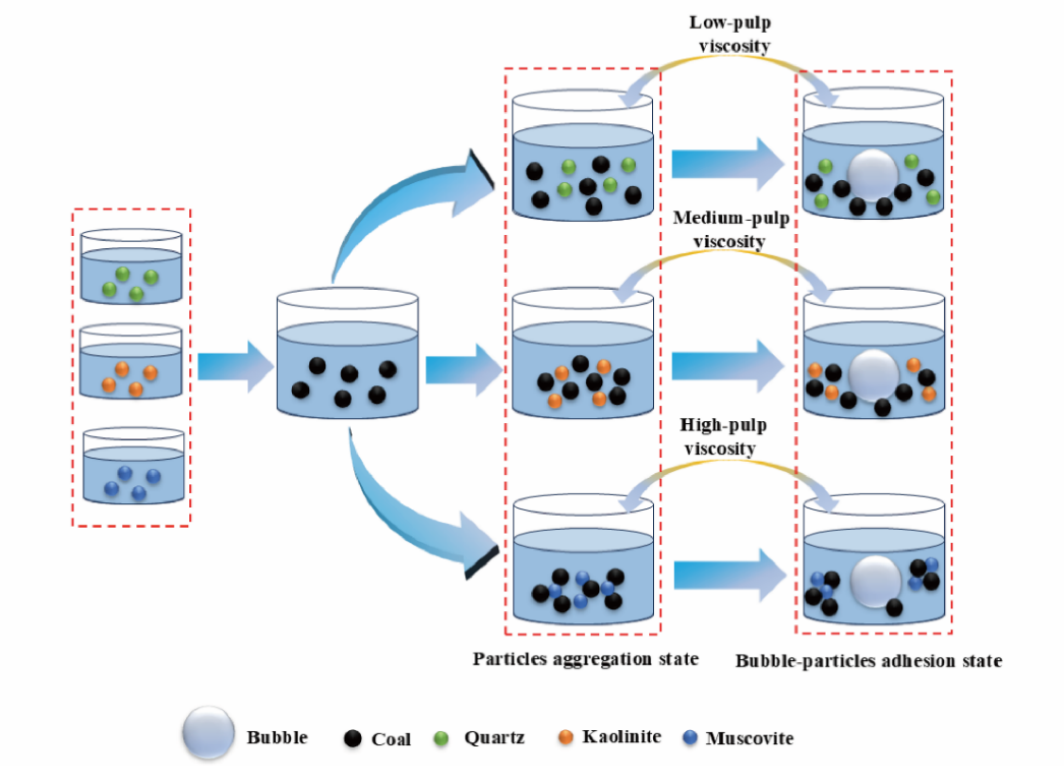

Fig. 10. Schematic mechanism of particle dispersion and bubble-particle adhesion states in pulp

4. Conclusions

(1) Different minerals have different effects on the apparent viscosity of coal slime. Apparent viscosity analysis revealed that coal-mineral slurries containing quartz, kaolinite, or muscovite exhibited shear-thickening behavior, characterized by increasing apparent viscosity with shear rate. Quartz minimally affected apparent viscosity, whereas kaolinite induced a moderate increase, and muscovite substantially enhanced it.

(2) The apparent viscosity difference directly affects the flotation performance. Flotation and bubble-particle adhesion experiments confirmed that the strongest inhibition was exerted by muscovite, followed by kaolinite, while quartz showed minimal impact. Notably, higher quantities of muscovite and quartz were recovered in the concentrate compared to kaolinite. Quantitative bubble loading capacity analysis revealed cross-sectional area reductions of 10.03% (quartz), 19.16% (kaolinite), and 30.14% (muscovite). Consequently, the adhesion suppression hierarchy—quartz (weakest) < kaolinite < muscovite (strongest)—correlated directly with flotation performance trends.

(3) Extended DLVO theoretical analysis revealed that as interparticle distance increases, the interaction energy between coal and both quartz and kaolinite transitions from attractive to repulsive. In contrast, coal-muscovite interactions maintained attractive energies across all separation distances, leading to aggregation between coal and muscovite particles and consequently adversely impacting coal flotation. These findings align with apparent viscosity behavior and flotation test results.

Acknowledgments

This research was funded by the National Natural Science Foundation of China (U24A2095).

References

BASNAYAKA, L., SUBASINGHE, N., ALBIJANIC, B., 2017. *Influence of clays on the slurry rheology and flotation of a pyritic gold ore*. Applied Clay Science 136: 230-238.

CHEN, L., ZHAO, Y., BAI, H., AI, Z., CHEN, P., HU, Y., SONG, S., KOMARNENI, S., 2020. *Role of montmorillonite, kaolinite, or illite in pyrite flotation: differences in clay behavior based on their structures*. Langmuir 36(36): 10860-10867.

CHEN, S., WANG, S., LI, L., QU, J., TAO, X., HE, H., 2018. *Exploration on the mechanism of enhancing low-rank coal flotation with cationic surfactant in the presence of oily collector*. Fuel 227: 190-198.

CHEN, W., CHEN, F., BU, X., ZHANG, G., ZHANG, C., SONG, Y., 2019. *A significant improvement of fine scheelite flotation through rheological control of flotation pulp by using garnet*. Minerals Engineering 138: 257-266.

CHEN, X., PENG, Y., 2018. *Managing clay minerals in froth flotationA critical review*. Mineral Processing and Extractive Metallurgy Review 39(5): 289-307.

CRUZ, N., PENG, Y., 2016. *Rheology measurements for flotation slurries with high clay contents - a critical review*. Minerals Engineering 98: 137-150.

CRUZ, N., PENG, Y., WIGHTMAN, E., XU, N., 2015. *The interaction of ph modifiers with kaolinite in copper-gold flotation*. Minerals Engineering 84: 27-33.

DAS, G. K., KELLY, N., MUIR, D. M., 2011. *Rheological behaviour of lateritic smectite ore slurries*. Minerals Engineering 24(7): 594-602.

DENG, J., YANG, S., LIU, C., LI, H., 2019. *Effects of the calcite on quartz flotation using the reagent scheme of starch/dodecylamine*. Colloids and Surfaces a-Physicochemical and Engineering Aspects 583.

FARROKHPAY, S., 2012. *The importance of rheology in mineral flotation: a review*. Minerals Engineering 36-38: 272-278.

FARROKHPAY, S., NDLOVU, B., BRADSHAW, D., 2016. *Behaviour of swelling clays versus non-swelling clays in flotation*. Minerals Engineering 96-97: 59-66.

GAO, L., LI, X., LYU, X., ZHU, X., 2024. *Advances and perspectives of green and sustainable flotation of low-rank/oxidized coal: a review*. Energy & Fuels 38(3): 1566-1592.

GAO, Y., ZHANG, G., WANG, M., LIU, D., 2018. *The critical role of pulp density on flotation separation of nickel-copper sulfide from fine serpentine*. Minerals 8(8).

GUO, H., HUANG, L., LIU, X., WANG, L., XIA, Y., CAO, Y., GUI, X., XING, Y., 2023. *Effect of different mass proportions of fine slime on the flotation performance of coal*. International Journal of Coal Preparation and Utilization 43(11): 1863-1884.

HU, P., LIANG, L., LI, B., XIA, W., 2019. *Heterocoagulation between coal and quartz particles studied by the mineral heterocoagulation quantifying system*. Minerals Engineering 138: 7-13.

HUANG, G., XU, J., GENG, P., LI, J., 2020. *Carrier flotation of low-rank coal with polystyrene*. Minerals 10(5).

JELDRES, R. I., URIBE, L., CISTERNAS, L. A., GUTIERREZ, L., LEIVA, W. H., VALENZUELA, J., 2019. *The effect of clay minerals on the process of flotation of copper ores - a critical review*. Applied Clay Science 170: 57-69.

KUMAR, K., ARORA, R., 2022. *Effect of additive on rheology of fine particles slurry suspension*. Materials Today. Proceedings 50: 1413-1416.

LI, G., DENG, L., CAO, Y., WANG, B., RAN, J., ZHANG, H., 2017. *Effect of sodium chloride on fine coal flotation and discussion based on froth stability and particle coagulation*. International Journal of Mineral Processing 169: 47-52.

LI, P., ZHANG, M., LEI, W., YAO, W., FAN, R., 2020. *Effect of nanobubbles on the slime coating of kaolinite in coal flotation*. ACS Omega 5(38): 24773-24779.

LI, Q., LIANG, L., TAN, J., XIE, G., 2022. *The influence mechanism of micron surface roughness on slime coating and bubble attachment on coal surface*. Minerals Engineering 189.

LI, Q., ZHANG, W., TAN, J., LIANG, L., XIE, G., 2023. *Mechanism of slime coating on coal surface with different metamorphic degrees*. Colloids and Surfaces a-Physicochemical and Engineering Aspects 675.

LI, X., ZHANG, Q., QIU, Y., LI, X., ZHAO, Y., XU, L., 2025. *Correlation between clay minerals, rheology, and flotation in the desulfurized pulp of high-sulfur bauxite*. Langmuir 41(21): 13166-13183.

LI, Y., XIA, W., PAN, L., TIAN, F., PENG, Y., XIE, G., LI, Y., 2020. *Flotation of low-rank coal using sodium oleate and sodium hexametaphosphate*. Journal of Cleaner Production 261.

LI, Y., XIA, W., WEN, B., XIE, G., 2019. *Filtration and dewatering of the mixture of quartz and kaolinite in different proportions*. Journal of Colloid and Interface Science 555: 731-739.

LI, Z., ZHAO, C., ZHANG, H., LIU, J., YANG, C., XIONG, S., 2019. *Process intensification of stirred pulp-mixing in flotation*. Chemical Engineering and Processing-Process Intensification 138: 55-64.

LIN, Q., MEI, Y., HUANG, W., ZHANG, B., LIU, K., 2022. *Understanding the role of polyvinylpyrrolidone on ultrafine low-rank coal flotation*. ACS Omega 7(12): 10196-10204.

LIU, D., ZHANG, G., GAO, Y., 2021. *New perceptions into the detrimental influences of serpentine on Cu-Ni sulfide flotation through rheology studies and improved the separation by applying garnet*. Minerals Engineering 171.

LIU, Z., CUI, Y., JIAO, F., QIN, W., WEI, Q., 2024. *Galvanic interaction between galena and pyrite in the presence of sodium lignosulfonate and its effects on flotation*. Langmuir 40(48): 25549-25557.

NI, C., BU, X., XIA, W., PENG, Y., YU, H., XIE, G., 2018. *Observing slime-coating of fine minerals on the lump coal surface using particle vision and measurement*. Powder Technology 339: 434-439.

SAJJAD, M., OTSUKI, A., 2022b. *Correlation between flotation and rheology of fine particle suspensions*. Metals 12(2).

SHANG, Y., SUN, C., 2023. *Effects of physical and physico-chemical factors on pulp rheology of smithsonite*. Physicochemical Problems of Mineral Processing 59(1).

TANG, J., ZHANG, Y., BAO, S., 2016. *The effect of Ca^{2+} and Mg^{2+} on the dispersion and flocculation behaviors of muscovite particles*. Minerals 6(3).

WANG, C., ZHANG, Q., MAO, S., QIN, S., 2020. *Effects of fine minerals on pulp rheology and the flotation of diaspore and pyrite mixed ores*. Minerals 10(1).

WANG, H., ZHU, H., ZHU, J., SHAO, S., HUANG, D., LIU, J., LI, T., 2020. *Effect of energy consumption on dispersion and recovery of coal slimes in a mechanical flotation cell*. Energy Sources Part a-Recovery Utilization and Environmental Effects 42(15): 1882-1890.

WANG, L., LI, C., 2020. *A brief review of pulp and froth rheology in mineral flotation*. Journal of Chemistry 2020.

WANG, Y., PENG, Y., NICHOLSON, T., LAUTEN, R. A., 2016. *The role of cations in copper flotation in the presence of bentonite*. Minerals Engineering 96-97: 108-112.

WANG, Z., MU, Y., ZHANG, M., CAO, Y., LI, C., 2024. *Effect of clay crystal structure on froth rheology in flotation*. Powder Technology 435.

XING, Y., XU, X., GUI, X., CAO, Y., XU, M., 2017. *Effect of kaolinite and montmorillonite on fine coal flotation*. Fuel 195: 284-289.

YAN, L., ENGLERT, A. H., MASLIYAH, J. H., XU, Z., 2011. *Determination of anisotropic surface characteristics of different phyllosilicates by direct force measurements*. Langmuir 27(21): 12996-13007.

YU, Y., MA, L., WU, L., YE, G., SUN, X., 2017. *The role of surface cleaning in high intensity conditioning*. Powder Technology 319: 26-33.

YU, Y., MA, L., XU, H., SUN, X., ZHANG, Z., YE, G., 2018. *DLVO theoretical analyses between montmorillonite and fine coal under different pH and divalent cations*. Powder Technology 330: 147-151.

ZHANG, M., CAO, Y., CHEN, Y., YU, W., 2017. *Influence of controlled dispersion on rheology of swelling clay suspensions in the presence of coal flotation reagents*. Physicochemical Problems of Mineral Processing 53(2): 1148-1160.

ZHANG, M., PENG, Y., 2015. *Effect of clay minerals on pulp rheology and the flotation of copper and gold minerals*. Minerals Engineering 70: 8-13.

ZHAO, L., ZHANG, Q., 2024. *Study of oleic acid-induced hydrophobic agglomeration of apatite fines through rheology*. Minerals Engineering 218.

ZHU, Z., ZHAO, B., WANG, J., ZHU, Y., SHENG, Q., LI, Z., ZHANG, N., YU, W., 2025. *Reduction of slime coating: effects of sodium silicate and sodium carbonate on lean coal flotation in sodium oleate system*. Journal of Dispersion Science and Technology 46(8): 1205-1215.